Indian J. Phys. **67B** (6), 511 – 525 (1993)

f' : its present and its future

Dudley Creagh
Department of Physics, University College, The University of New South Wales, Australian Defence Force Academy, Canberra, ACT 2600, Australia

Abstract : This paper compares measurements of f' made using interferometer, absorption, reflectivity and deviation of a prism techniques at, or near, the K-absorption edges of calcium, nickel, copper, the $L2$- and $L3$-absorption edges for gold, and the K-absorption edge of uranium. It considers the effectiveness of the present scalar definition of f' and comments on recent attempts to give a tensor formalism for f'

Keywords : Dispersion correction, scaler definition, tensor formalism

PACS Nos. : 07.60 Ly, 11 20 Fm

1. Introduction

I do not wish here to give a comprehensive resume of the history of the measurement and calculation of the real part of the (anomalous) dispersion correction. Nor have I the space to give a comprehensive exposition of the techniques of measurement used and the details of the several methods for calculating f'. These have been discussed elsewhere [1].

Rather, I wish to compare recent theoretical calculations and experimental data from experiments performed in the past decade. The extent to which the experimental data and the theoretical predictions accord with one another will be discussed.

The atomic form factor and its associated dispersion corrections f' and f'' have hitherto been considered to be scalar quantities. In a later section of this paper I shall address the implications of recent attempts to develop a tensor formalism for f'.

2. Theoretical and experimental methods

The impetus to study extensively the dispersion corrections was given by Bijvoet *et al* [2] in a paper which described how the X-ray dispersion effects predicted by Waller [3] and extended by Honl [4] could be used to resolve the phase problem in the solution of crystal structures. The vigorous interest in anomalous dispersion and its use in experimentation led to the organisation of the Intercongress Conference on Anomalous Scattering, the proceedings of which recorded in [5].

At this conference the use of an X-ray interferometer and synchrotron radiation source to determine f'' at an absorption edge was reported for the first time (Bonse and Materlik). The new relativistic dipole theory of Cromer and Liberman [6] was brought to the attention of crystallographers and replaced the non-relativistic theories [7] based on the theory of Hönl [4]. The Cromer and Liberman (RDP) approach was to remain the standard theoretical data set for almost two decades [7].

Improvements in computing equipment and software and refinements to the theoretical approach led to the relativistic multipole (RMP) theory of Creagh and McAuley which is the basis for the tables in International Tables for Crystallography, Vol C [1]. Using a more elegant approach Kissel *et al* [9] developed an S-matrix formalism to calculate Rayleigh scattering amplitudes.

All of these theories have features in common. They attempt to calculate the scattering amplitudes for elastic scatter of X-rays by atoms which are isolated and spherical. Transitions which occur are assumed to have their origin in transitions between atomic energy levels or atomic energy levels and the continuum only are considered. No states arising from the presence of neighbouring atoms are taken into account.

In terms of the form factor formalism all seek to write the scattering power of such an atom as

$$f = f_0 + f' + if'' \tag{1}$$

where f_0 is the atomic form factor and f' and f'' are the real and imaginary parts of the atomic scattering factor respectively. The imaginary part is proportional to the atomic scattering cross section σ.

In the non-relativistic case the atomic form factor f_0 which arises from the comparison of the scattering power of the free atom with that of a Thomson electron is given by

$$f_0 = 4\pi \int^{\infty} \rho(r) \frac{\sin \Delta r}{\Delta r} r^2 dr. \tag{2}$$

Here $\rho(r)$ is the electron density and $\Delta = \boldsymbol{k}_f - \boldsymbol{k}_i$, where $\boldsymbol{k}_f$ and $\boldsymbol{k}_i$ are respectively the final and initial wavevector. In the relativistic case the modified relativistic form factor is used. For the scattering power of the i-th energy level

$$g_i = 4\pi \int_0^{\infty} \rho_i(r) \frac{\sin \Delta r}{\Delta r} \frac{mc^2}{(E_i - V(r))} r^2 dr. \tag{3}$$

The additional term in eq. (3) is inserted to take into account relativistic binding effects.

The theories differ also in the techniques used to evaluate f'' The nonrelativistic and relativistic theories differ in the nature of the wavefunctions chosen for use in the calculations. However there is a further difference between these two theories. The performance of a Kramers-Kronig transformation on the atomic absorption cross section data leads to a term in the expression for f' in the relativistic case not present in the non-relativistic case. This corresponds to the matrix element for forward scatter at infinite photon energy.

$$f' = f^{+} + f^{R} \tag{4}$$

The term f^{+} has the form a Kramers-Kronig integral

$$f^{+} = \frac{r_0}{\pi hc} \wp \int_{mc^2}^{\infty} \frac{\left(E^{+} - E_1\right)^2 \sigma\left(E^{+} - E_1\right)}{\left(h\omega\right)^2 - \left(E^{+} - E_1\right)^2 + i\Gamma\left(E^{+} - E_1\right)/2} dE^{+} \tag{5}$$

where E^{+} ($= mc^2 + E^{+}$) represents a positive energy value and E_1 ($= mc^2 + E_1$) is the energy of the bound state for the electron. Γ is the total radiative linewidth for the relevant absorption edge.

Application of a relativistic dipole theory [6,8] gives the value of f^R as

$$f^R = \frac{5}{3}\frac{E_{tot}}{mc^2}. \tag{6}$$

If, however, a multipole, rather than a dipole, expansion is taken into account and full account is taken of retardation effects,

$$f^R = E_{tot}/mc^2. \tag{7}$$

Note that the values given in eqs. (6) and (7) are constant for a particular atom, being related to the total self-energy of the atom E_{tot}. Note also that there is little difference between values of calculated by Cromer and Liberman [6,8] and Creagh and McAuley [1].

The S-matrix approach has a completely philosophy and this difference between the theories has been reviewed by Creagh [10]. An important feature of the S-matrix theory is that it can take into account polarization of the X-rays, whereas the RDP and RMP theories were developed for averaged polarization. Furthermore the S-matrix theory can take into account the angle of scattering whereas the RDP and RMP theories were developed solely for forward scatter. Some indication of the differences in predications of these theories is given in Table 1.

The S-matrix and RMP values are in general agreement with one another. There are significant differences between the NR and RDP values and the S-matrix and RMP values.

Of the experimental data available the most reliable and consistent data sets have been taken using the Ångstrom ruler interferometer pioneered by Hart [11]. Data identified as

interferometer data in the figures given in this paper have been taken with Ångstrom rulers. These interferometers are transmission devices and therefore can be used to measure X-ray

Table 1. Comparison of theoretical predictions of the real part of the forward scattering amplitude.

Atom	Radiation	f_0+f'			
		NR	RDP	SMAT	RMP
^{13}Al	CrKα_1	13 376	13.316	13.324	13.326
	CuKα_1	13 235	13.203	13.211	13.213
	AgKα_1	13.078	13.020	13.028	13.041
^{30}Zn	CrKα_1		29.314	29.381	29.383
	CuKα_1		28.383	28.450	28.451
	AgKα_1		30.232	30.299	30.313
^{32}Ge	CrKα_1	30 20	31.538	31 617	31.614
	CuKα_1	31.92	30.837	30.916	30.911
	AgKα_1	32.14	32.228	32.307	32.302
^{73}Ta	AgKα_1		71 994	72.634	72.617
^{82}Pb	AgKα_1		80.012	80.882	80.832

absorption as well as refractive index. This allows one to calculate f' independently using the Kramers-Kronig transform [12,13].

Many of the recent determinations of f' have had their genesis in extended X-ray absorption fine structure (XAFS) measurements. These measurements are transmission measurements and are, in principle, easy to perform. Problems in making these measurements have been discussed by Creagh [14].

Two early techniques for measuring the refractive index of a material and therefore, f', have been recently revived. The first, which measures the angle of deviation of the X-ray beam using a Bonse-Hart triple axis diffractometer, has been used by Ishida [15] and Katoh *et al* [16] for measurements in the vicinity of the K-absorption edge of germanium. Good agreement was found with the RMP theory (see [14]).

In the second and reflectivity of the sample is measured in the region of the angle of total external reflection. This technique is most useful in measuring f' in heavily absorbing materials [17].

3. Results

Experimental values for f' for calcium are plotted as open circles in Figure 1 as a function of the wavelength of the incident X-ray. These values were deduced from measurements by

Creagh of refractive indices of calcium fluoride specimens using an X-ray interferometer, and are the open circles in Figure 1. Also shown are the values calculated using non-relativistic

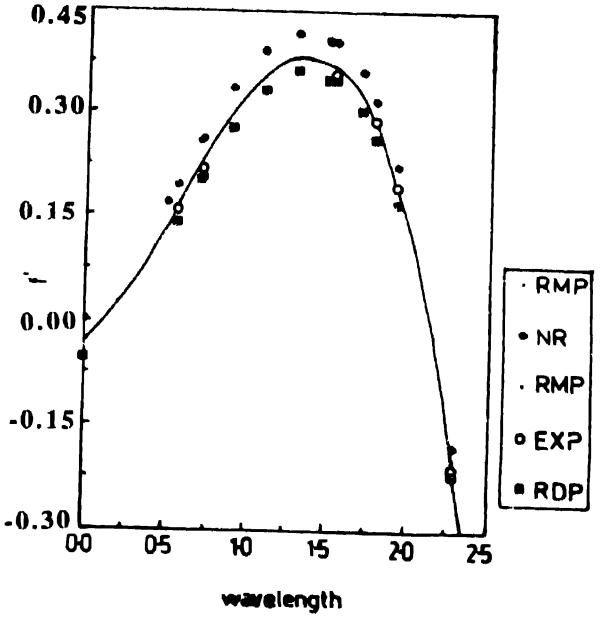

Figure 1. *f′* data for calcium, measured with an interferometer, (open circles) are compared with the predictions of the NR (diamond), RDP (solid square) and RMP (solid line) theories.

(NR) and relativistic dipole (RDP) theories. The agreement between the RMP theory (solid curve) and the experimental values is quite good, being typically 5%.

Of the three theories the RMP theory gives the best fit to the experimental points. It is possible to show the S-matrix values on this graph because they lie close to the RMP values. (Add 0.003 to all the RMP values).

In Figure 2, f' measurements using interferometric [12], reflectivity [18] and absorption data are plotted as a function of energy in the vicinity of the K-absorption edge of copper, and compared with the RMP theory. The absorption data (open circles) was taken by Creagh and Oyanagi [19] and the f' values were deduced by calculating the Kramers-Kronig integral of the absorption cross section, and then adding to the values obtained the appropriate relativistic correction. Values interpolated from the interferometer experiments of Begum *et al* [12] are shown as crosses and the reflectivity measurements [18] are shown as diamonds.

The agreement on the low energy side of edge between the various experiments and the RMP predictions are quite good. However, at energies above the edge significant differences exist between the several experimental data sets. The differences are due to XAFS modulations and are caused by differences in energy bandpass for the experimental system used.

None of the theories pretend to have any validity in this region. They can deal only with scattering from isolated atoms. In condensed matter there are interactions of the ejected

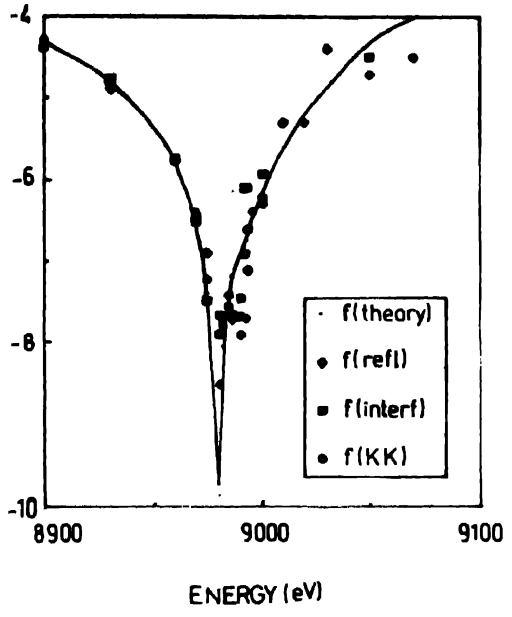

Figure 2. f' data for copper, deriving from interferometer (+), reflectivity (◆) and absorption data (o), are compared with the RMP theory (solid line).

photoelectrons with the atoms in the neighbouring shells to the atom site from whence the electron was ejected. As well, energy levels exist which do not exist in the isolated atom case.

One does not, however, need to move far from the edge for good agreement between theory and experiment to occur exist once more.

A similar situation exists for the f' data taken for nickel (Figure 3). Here XAFS effects change the shape of the curve significantly on the high energy side of the edge. As before, these modulations cannot be predicted by existing theories. Agreement between theory and experiment becomes good away from the edge.

For gold the effect of XAFS on the measurements of f' in the neighbourhood of the L2-absorption edge is not pronounced (Figure 4). Below the absorption edge energy agreement between the RMP theory and experiment is acceptable. Above the edge, quite significant deviations are found, certainly due to electronic transitions and interactions for which the isolated atom theory cannot take account. In the vicinity of L3-edge agreement between theory and experiments is quite acceptable (Figure 5).

Figure 6 shows a comparison between interferometic measurements by Hart *et al* [20] for uranium in the vicinity of its K-absorption edge and two theoretical curves. The solid

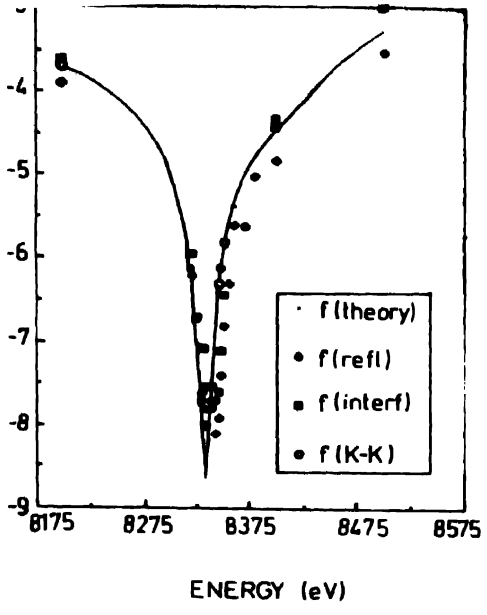

Figure 3. *f″* as a function of X-ray energy in the neighbourhood of the *K*-edge of nickel. Data from [12] are shown as a cross. Data from [18] are shown as a diamond. Absorption results are shown as an open circle. The RMP theory is shown as a solid line.

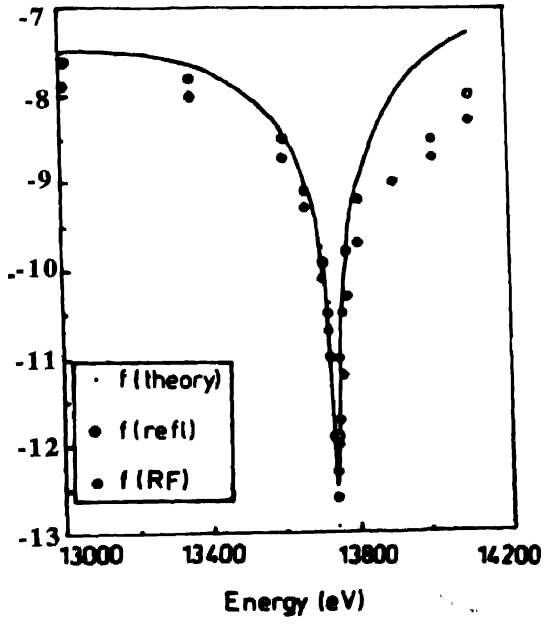

Figure 4. *f″* as a function of X-ray energy in the neighbourhood of the *L*2-absorption edge of gold. Data from [18] is shown as a diamond. Other measurements (Creagh) are shown as a circle. The RMP theory is shown as a solid line.

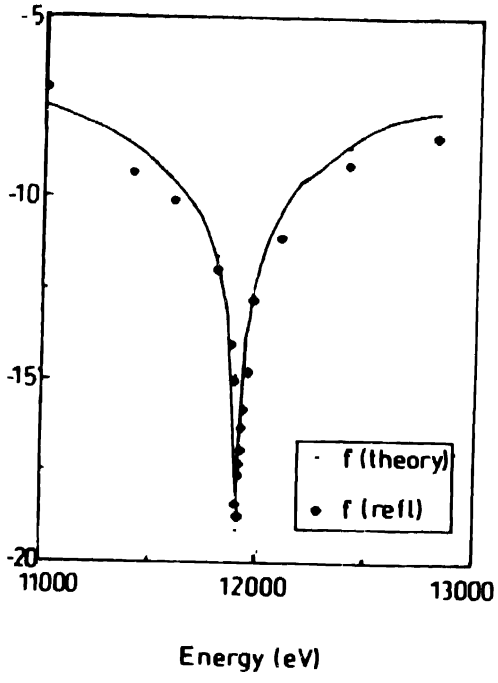

Figure 5. f' as a function of X-ray energy in the neighbourhood of the $L3$-edge of gold. Data from [18] is compared with the RMP theory

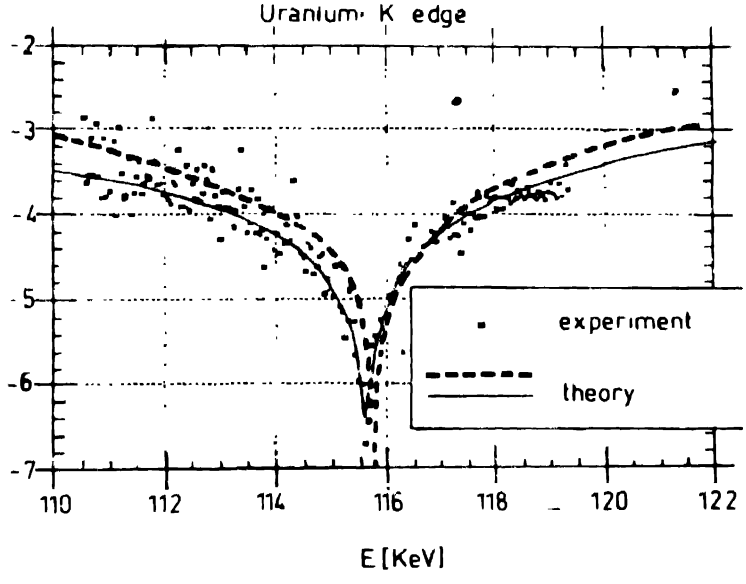

Figure 6. f' measurements for uranium in the vicinity of its K-absorption edge [20]. The solid line was calculated using a semi-empirical theory [21]. The dotted line was calculated using the RMP theory [1]

curve was calculated using the semi-empirical theory of Parratt and Hempstead [21]. The dotted curve is calculated using the RMP theory of Creagh and McAuley [1].

A discrepancy exists between the energy of the *K*-absorption edge measured using an interferometer and the values used in the theoretical calculation (taken from [22]). This may be due to internal oxidation of the uranium specimen. It is well known that the oxidation state of an element alters the energies at which its absorption edges occur.

The effect of XAFS is apparent on the high energy side of the absorption edge. Regrettably the experimental data does not extend to sufficiently high energies to see whether good agreement between theory and experiment is found when the XAFS oscillations cease to exist.

4. Discussion

From a systematic comparison of theories, and the intercomparison of theories and experiment there can be little doubt that the RMP theory [1] gives a good description of the experimental results and is demonstrably superior to the RDP and the NR theories.

The difference between the RMP and the *S*-matrix theories is small and constant with energy for a particular element. For example, for all energies :

for Z = 20 the addition of 0.002 to the RMP values yields the *S*-matrix value;

for Z = 50 the addition of 0.030 to the RMP values yields the *S*-matrix value;

for Z = 92 the addition of 0.214 to the RMP values yields the *S*-matrix value.

Of the two, the *S*-matrix theory is the more complete because it can account for the change in polarization of the incident X-ray and calculate angles of scatter other than forward scatter. However it requires considerable computing power. In contrast the RMP programme can run in a modern personal computer, although at present it is not in a user-friendly form.

Users at synchrotron radiation source require scattering data for the energy they are currently using whereas users of conventional X-ray systems use the characteristic 'emission' radiation from target materials for which the photon energy is well known.

There is a need therefore for both a convenient computer programme and a tabulated data set.

The extent to which the various experimental techniques agree with one another is remarkable given the problems presented by working at the absorption edges of materials. Of the techniques the X-ray interferometer technique is the best for elements having a low atomic number. The reflectivity method becomes useful for elements with large atomic weights because of the high absorption of these materials.

Experimental problems are common to all techniques and are listed below :

* The energy of the incident photon may not be known to sufficient precision, because of monochromator angle inaccuracies. The energy band pass for the monochromator system may also be excessive.
* The detector may have insufficient resolution to discriminate between Rayleigh and other scattering processes.
* Experience has shown that a wide range of deficiencies may be found in the way samples are prepared. Inhomogeneity in composition, impurities, surface roughness (transmission samples have to be thin to allow an adequate transmitted intensity and reflectivity samples have to be smooth to reduce nonspecular reflection), the presence of oxide coatings, contrive to reduce the accuracy and reproducibility of experiments.

The RMP theory which forms the basis for the tables in International Tables for Crystallography Volume C gives an acceptable description of Rayleigh scattering even close to an absorption edge For a range of typically 200 eV above an absorption edge the XAFS modulations influence the values of f' in condensed matter. Despite this the isolated atom (form factor) theory gives a good first order description of the scattering process.

The values given by S-matrix theory can be deduced by adding a small constant to the RMP values [19].

The results of measurements using different experimental techniques are largely in agreement with one another. In any experiment great care must be taken to ensure that deficiencies in sample preparation do not mask the true value of the measurement.

5. f' As a tensor : is this concept valid ?

The form-factor formalism, as it is applied in crystallography, is one of model making and model comparison.

A crystal structure is thought of as being the summation of its individual atom components with no account being taken of chemical bonding.

Within a unit cell of crystal structure each atom will occupy a particular site, the j-th atom being associated with the position u, v, w within the unit cell. For a Bragg reflection h, k, l from the crystal the contribution to scattering of the unit cells as a whole is given by the geometrical structure factor

$$F_{hkl} = \sum f_j \exp\left(2\pi i\left(hu + kv_j + lw_j\right)\right). \tag{8}$$

The intensity of that Bragg reflection will be proportional to $|F_{hkl}|^2$.

Thus, for example, the intensity of scattering from a real crystal can be compared with that for model structures. If the comparison of intensities is good for one model and not for

another, the assumption is made that the structure of the crystal predicted by the first model was correct, whereas the second was not correct. This procedure is important in the solution of large single crystals, *e.g.* proteins, macromolecules, and in powder diffraction.

An example of model fitting using Rietveld modelling, based on values of f calculated using the RDP programme is shown in Figure 7a. In this the powder diffraction data taken by Will [23] for Mg_2GeO_4 is compared with the theoretically computed data. Deviations from fit are due in part to the inaccuracy caused by using an RDP rather than an RMP calculation for f'.

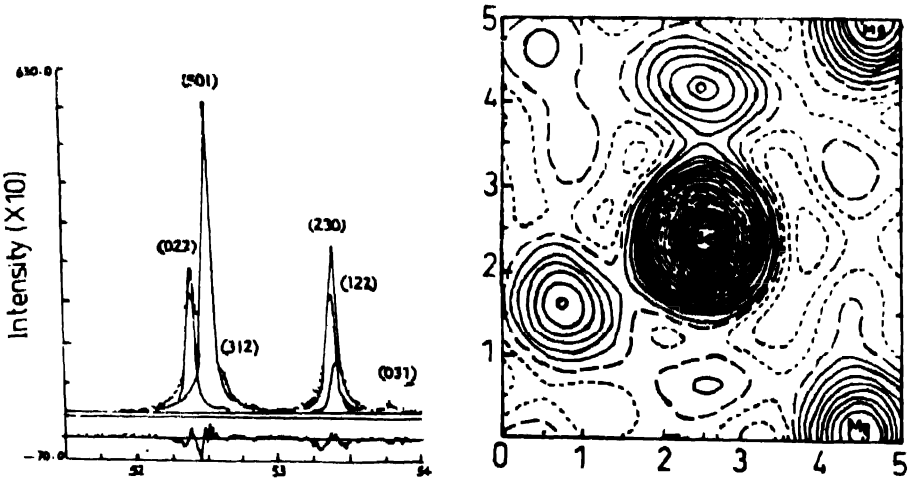

Figure 7. Data from Will [23] for Mg_2GeO_4 (a) Rietveld fit to the experimental powder diffraction data (b) Electron density map showing the covalent bonding between the Ge and O atoms, and the ionic bonding between the Ge and Mg atom

If the structure is known, then the deviation of the experimental intensity distribution from that of the model gives information about the distribution of charge between lattice sites.

This follows from the fact that the Fourier transform of eq. (8) gives directly the electron density $\rho(xyz)$ as function of position xyz in the crystal.

$$\rho(xyz) = \frac{1}{V}\sum_{hkl} |F_{hkl}| \exp(i\alpha_{hkl}) \exp[-2\pi i(hx + ky + lz)]. \tag{9}$$

Here, V is the volume of the unit cell and $F_{hkl} = |F_{hkl}| \exp(i\alpha_{hkl})$.

By subtracting from the measured $\rho(xyz)$ the values calculated using the model structure for the material and the atomic form factors calculated for isolated atoms the distribution of charge within the unit cell due to bonding effects can be deduced.

The difference electron density map for the Mg_2GeO_4 specimen whose diffraction is shown in Figure 7a is plotted in Figure 7b.

It is clear that surplus electron density exists between the germanium and oxygen atoms, and one can clearly see that the germanium is covalently bonded to the oxygen and ionically bonded to the magnesium.

This structure, then, has been solved, both for the positions of the atoms and the nature of the bonding between atoms.

The structure could not have been solved so exactly if the form factor formalism were not a good first approximation. Nor could the electron density map be determined so exactly unless the scalar values of f were calculable to sufficient precision.

But the mere existence of ligands between atoms implies that now the nature of nearest neighbour interactions must impose some symmetry on the scattering process and this is determined by the local site symmetry, on the scattering process.

We have already seen some of these effects in Figures 2 to 6, where the XAFS oscillations, which are due to interaction of the ejected photoelectron with electron density due to neighbouring atoms, have an effect on the scattering power of the atom in the vicinity of its absorption edge.

In general the effect of XAFS oscillations are small compared to f. For example, near the gold $L2$-edge at a photon energy of 14 KeV the deviation of the measured curve from the theoretical curve is about 1 electron. This implies that the gold atom scatters as though it has 70 electrons rather than 69 electrons. Since the intensity is proportional to the square of the f value the difference between the experimental and theoretical cases is about 3%.

It is possible therefore to treat the XAFS modulation as a perturbation to the isolated atom scattering. Values of f' due to the XAFS can be calculated from programmes like Rehr's FEFF programme [24], and these can be added to the RMP values to give almost exact agreement between theory and experiment.

My point is that the XAFS rarely contributes more than a couple of precent to the scattering, and even then acceptable techniques exist to compensate for any problems they may cause.

But, with the advent of the new generation synchrotron radiation sources with their high degree of polarization and their high brilliance, it is possible to detect effects which have hitherto been inaccessible to experimentalists. These are so-called tensor effects which arise from local crystal symmetry effects in the neighbourhood of an anomalously scattering atom. The first such effects, X-ray circular dichroic effects, were observed by Templeton and Templeton [25], and they have developed further their notions in later papers [26,27].

It must be stressed here that these tensor effects are specific to particular crystal structures. They reflect the nature of the symmetry of the crystal field in those particular

structures. They lead to the acquisition of further knowledge once the structure of the system is known *i.e.* after the application of the scalar model.

A further elaboration of the tensor approach has been given by Kirfel and Petkov [28]. In the dipole approximation the atomic scattering factor formalism can be written in terms of symmetric second rank tensor $\|f'\|$ and $\|f''\|$ which have to be compatible with the site symmetry of the atom species under investigation.

$$\|f'(\omega, \Delta)\| = \|f_0(\Delta)\| + \|f'(\omega)\| + i\|f''(\omega)\|. \tag{10}$$

Using this concept the structure factor tensors are different in the crystal system $\|F(\Delta)\|$ or the diffractometer system $\|F(\Delta)_D\|$. Various factors than enter into the determination of the intensity reflection. These may include radiation energy ($E = \hbar\omega$) and scattering angle θ, the orientation of the crystal with respect to the scattering vector, the polarization of the incident radiation, all of which may be controlled by the experimenter, and the existence of resonance scattering, and deviations from stoichiometry, which are functions of the sample.

Because of the tensor nature of the crystalline bonding, reflections may be observed in space groups for which the reflection is forbidden on general symmetry arguments.

Higher order tensor effects are observable in the neighbourhood of the absorption edges for a number of rare earth and transition metal elements. These are typically fourth rank tensors associated with the scattering of photons from electron spins in ferromagnetic and anti-ferromagnetic materials. The possibility of such scattering was first predicted by Platzman and Tsoar [29] and later observed by de Bergevin and Brunel [30]. Subsequently considerable research has been carried out by Monkton *et al* [31] and further commentary has been given by Creagh [32].

More recent theoretical discussion of this phenomenon has been given by Blume [33]. The enhancements to magnetic X-ray scattering near an absorption edge, in particular in the near edge (XANES) region are strongly related to the site symmetry of the scattering atom. The scattering is strongly polarization dependent and is strongest at the *M*-shell edges of rare earths and actinides.

Despite the fact that these effects are readily detectable effects associated with interesting physical effects, the contribution to the total scattering cross section of the magnetic scattering is at best 0.001%.

6. Comments

The scalar representation for the atomic form factor and its dispersion correction is required to solve both the crystal structure and electron distribution in crystals. At the present state of knowledge errors in f are less than 0.2% even for transuranic elements.

Once the structure is known it is then possible to redefine the atomic structure factor slightly to extend its use in experiments involving X-ray circular dichroism, the Faraday effect, magnetic scattering and so on. This leads to a tensor formalism where the tensor terms are specific to the site symmetry of the principal scattering atoms. These may be thought of as additional additive terms in the scattering process, which act to add some directionality to the atomic scattering factor.

This does not imply that f' and f'' can be treated as refinable variables in crystal structure analysis.

Acknowledgments

This work was supported in part by the Australian Research Council. The author acknowledges the considerable experimental assistance given by Dr H Oyanagi, the continuing encouragement given by Professor M Hart and Dr J Hubbell and fruitful discussions with Dr M Blume.

References

[1] D C Creagh and W J McAuley 1992 in *International Tables for Crystallography* **Vol C** ed A J C Wilson (Dordrecht : Kluwer) p 206

[2] J M Bijvoet, A F Peerdeman and A Van Bommel 1951 *Nature* **168** 271

[3] I Waller 1928 *Z. Phys* **51** 213

[4] H Honl 1933 *Z Phys.* **84** 1

[5] S Ramaseshan and S C Abrahams (eds) 1975 *Anomalous Scattering* (Copen Hagen · Munksgaard)

[6] D T Cromer and D Liberman 1970 *J Chem Phys.* **53** 1891

[7] H Wagenfeld 1975 in *Anomalous Scattering* eds S Ramaseshan and S C Abrahams p12

[8] D T Cromer and D Liberman 1974 in *International Tables for Crystallography* **Vol IV** eds J Ibers and W C Hamilton Chap 2.3

[9] L Lissel, R H Pratt and S C Roy 1980 *Phys. Rev* **A22** 1970

[10] D C Creagh 1989 *Aust J Phys* **43** 487

[11] M Hart 1968 *J. Phys* **D1** 1405

[12] R Begum, M Hart, K R Lea and P Siddons 1986 *Acta Crtyst.* **A42** 456

[13] U Bonse and A Henning 1986 *Nucl. Instrum. Meth.* **A246** 814

[14] D C Creagh 1990 *Nucl. Instrum. Meth.* **A295** 417

[15] K Ishida 1990 cited in *Nucl. Instrum Meth* **A295** 422

[16] H Katoh, H Shimakura, T Ogawa, S Hattori, Y Kobayashi, U Umezawa, T Ishikawa and K Ishida 1985 *J Phys. Soc Jpn* **A5** 881

[17] F Stanglmeier, B Lengeler, W Weber, H Göbel and M Schuster 1992 *Acta Cryst.* (to be published)

[18] D C Creagh and H Oyanagi 1990 (unpublished)

[19] L Kissel and R H Pratt 1990 *Acta Cryst.* **A46** 170

[20] M Hart, J B Hastings, D P Siddons and U Lienert 1992 *Abstracts for ICAS Conference (Malente)* p 38

[21] L G Parratt and C F Hempstead 1954 *Phys. Rev.* **94** 1593

[22] J A Bearden 1967 *Rev. Mod. Phys.* **39** 78

[23] G Will 1988 *Aust. J Phys.* **41** 283

[24] J J Rehr and R C Albers 1990 *Phys. Rev.* **B41** 8139

[25] D H Templeton and L Templeton 1982 *Acta Cryst.* **A38** 62

[26] D H Templeton and L Templeton 1986 *Acta Cryst* **A42** 478

[27] D H Templeton and L Templeton 1987 *Acta Cryst* **A43** 573

[28] A Kirfel and A Petkov 1992 *Acta Cryst* **A48** (in press)

[29] P M Platzman and N Tsoar 1970 *Phys. Rev* **B2** 3556

[30] F de Bergevin and M Brunel 1972 *Phys Rev Lett* **39** 141

[31] D E Monkton, D Gibbs and J Bohr 1986 *Nucl Instrum Meth.* **A246** 839

[32] D C Creagh 1988 *Aust. J Phys* **41** 155

[33] M Blume 1992 *Abstracts for ICAS Conference (Malente)* 12